International Journal of Energy Economics and Policy

ISSN: 2146-4553

available at http: www.econjournals.com

International Journal of Energy Economics and Policy, 2024, 14(4), 590-598.

Multi-step Natural Gas Price Forecasting using Ensemble Empirical Mode Decomposition and Long Short-Term Memory Hybrid Model

Herry Kartika Gandhi*, Ispány Márton

Faculty of Informatics, University of Debrecen, Postcode 4028, Hungary. *Email: herry.kartika@inf.unideb.hu

Received: 01 February 2024 **Accepted:** 30 May 2024 **DOI:** https://doi.org/10.32479/ijeep.16053

ABSTRACT

With the characteristic of natural gas as a clean, non-toxic, and valuable energy source, its use has been increasing in recent years. Thus, maintaining stable natural gas security requires a reliable long-step price forecasting indicator with less error. We propose a hybrid theory of Ensemble Empirical Mode Decomposition (EEMD) with Long Short-Term Memory (LSTM) to perform multi-step forecasting focusing on 30-90 steps of the daily Henry Hub natural gas price as a dataset. Using four widespread error measurements, the proposed model provides excellent results compared to no-decomposition as the benchmark model. The proposed model provides 50% lower error results than the single LSTM. EEMD_LSTM brings values below 10 in the MAPE indicator, even up to 90-step prediction. The Diebold-Mariano test also confirms that EEMD_LSTM outperforms the single LSTM on every step with the majority of 90% confidence level. We also simulated the model by analysing the box and whiskers plot of RMSE, which shows that the variance of predicted values ranges between 1.11%. These results show that the proposed forecasting model provides robust results for the case of medium-term natural gas prices with excellent forecasting results.

Keywords: Natural Gas Price, Hybrid Forecasting, EEMD, Decomposition, LSTM
JEL Classifications: C53, Q41, Q47

1. INTRODUCTION

In the context of the Paris Agreement (United Nations, 2015), where countries aim to reduce global carbon emissions by 30% by 2030, the role of natural gas (NG) as one of the key alternative energy sources to reduce the role of crude oil and coal becomes very important. NG has the advantages of being safe, efficient, and reliable. NG emits much lower carbon dioxide, nitrogen, and sulfur levels than other fossil fuel sources. As a result, the global use of NG shows a significant increase from 1998 to 2022 (Figure 1), during which time the use of NG has almost doubled (Statista Search Department, 2023) and reached 4 trillion cubic meters in 2022. In addition, natural gas is one of the top three energy sources in the world, with the most significant increases in the United States, South America, Asia, and Europe. However, although the use of NG is very similar around the world, the highly volatile price changes can affect the sensitivity of society and the decisions of buyers regarding NG installations and contracts over a long period (Elgharbawy, 2020; Melikoglu, 2013; Zamani, 2016).

Changes in the value of natural gas price (NGP) are influenced mainly by the supply and demand in the market. Price forecasting is an essential tool in creating a market integration system to anticipate uncontrolled demand fluctuations in the future. NGP forecasting is an early indicator in NG supply management to balance demand buyers and maintain uncontrolled inflation (Tamba et al., 2018). A reliable forecasting method can reduce the error gap, create good supply planning, avoid inflation, and improve energy security in the future.

Figure 1: NG consumption worldwide (In billion cubic meters) (Statista Search Department, 2023)

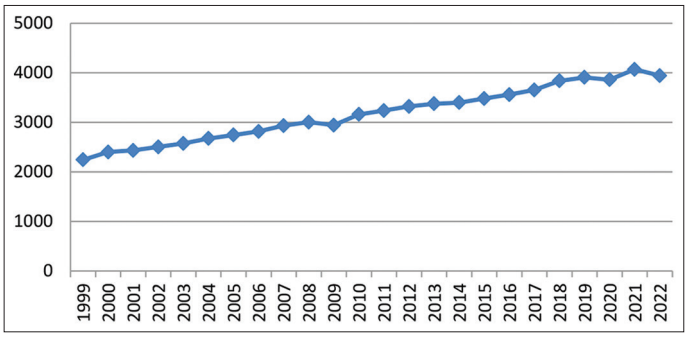

Price forecasting is one of the methods that continue to grow, and the latest method that is now getting much attention is Artificial Intelligence (AI). One of the popular methods is Deep Learning (DL) (Cordoni, 2020; Livieris and Pintelas, 2022). DL is a quantitative method based on the concept of neurons working in the human brain, where each neuron can self-learn to detect input data and try to analyse its relationship with the given output in the learning process. AI has a non-linear mechanism that uses an activation function not owned by other predictive processes; that function is to determine how much each neuron influences other neurons to provide prediction to the neuron output. Some applications of DL are as follows: Ramyar and Kianfar (2019) used an artificial neural network (ANN) for crude oil prices forecasting, which gave better results than the vector autoregressive model. Sehgal and Pandey (2015) also developed a feed-forward ANN, which gives more satisfactory results when compared with the machine learning concept of the support vector machine (SVM). The latest development of the ANN concept is LSTM; this model has been applied by several researchers, including Lu et al. (2021), who combined variable selection LSTM for the crude oil price, and Zhang et al. (2022), who used hybrid EMD-LSTM for the case of variation of electron flux. Among other deep learning models, LSTM has the advantage of combining the influence of long-term and short-term data in one model without causing vanishing or exploding gradients that can occur.

One of the most popular forecasting development concepts today is the hybrid decomposition model (Monjoly et al., 2019; Ozkan and Karagoz, 2015; Perone, 2022), where decomposition techniques are applied together with forecasting models to achieve better forecast accuracy results. Examples include Li et al. (2018), who used Ensemble Empirical Mode Decomposition (EEMD) with random forest to improve the accuracy of daily electricity consumption forecasts. In addition, Wang et al. (2015) combined EEMD and ARIMA to improve the accuracy of forecasting models on annual time series data. EEMD can decompose the initial data into each part according to its frequency, so the decomposition output has a smooth pattern that is easier to analyse further. Our concern is to use the EEMD decomposition to break the original data into several more structured patterns so that the forecasting model can better understand the inherent features of the data.

Based on some of our explorations, NGP forecasting studies are still relatively rare, especially those related to quantitative forecasting analysis. Table 1 shows examples of some NGP forecasting studies; in this journal, we use hybrid EEMD with a combination of LSTM. In this case, most forecasting models use a single-model forecasting system. In addition, the forecasting step is still in the small step range of 1-10 days ahead (Čeperić et al., 2017; Fan et al., 2022; Liu and Sun, 2019; Yan et al., 2018), while in this study, we propose longer ranges of step forecasting. Therefore, the objectivity of this study is [1] to use the EEMD decomposition technique as part of hybrid NGP forecasting, [2] to use deep learning LSTM model for forecasting tool, and [3] to compare multi-step forecasting from 30 to 90 days ahead to prove how good and robust this forecasting model is.

The structure of this journal starts with chapter 1 (Introduction), which describes the background of this forecasting study. This is followed by chapter 2, which describes the theory of decomposition and forecasting as well as the stages of application and mathematical formulation. Chapter 3 contains the data description and input method for the forecasting model; chapter 4 contains the data analysis and graph visualisation; and chapter 5 is the conclusion and future potential project.

2. LITERATURE REVIEW

Let x_t be the data set in the historical period t, with $t = 1,2,\ldots,T$, so for one-step forecasting: $= \hat{x}_{T+1}$, we formulate the forecasting model as: $\{ üüüü_t) = \hat{}_{T+1} \mid {}_t = {}_1, {}_2,\ldots, {}_T \}$. While n-step forecasting, where n = number of outputs, can be formulated as

$$\left\{ f\left(x_t\right) = \hat{x}_{T+1}, \hat{x}_{T+2}, \ldots, \hat{x}_{T+n} \mid x_t = x_1, x_2, \ldots, x_T, \hat{x}_{T+1}, \ldots, \hat{x}_{T+n} \right\} \quad (1)$$

2.1. Ensemble Empirical Mode Decomposition (EEMD)

Huang et al. (1996) first introduced Empirical Mode Decomposition (EMD) (the forerunner of EEMD), which can separate quantitative data into parts to gain an understanding of its inherent features. This technique can help understand non-linear and non-stationary data. EMD generates multiple intrinsic mode functions (*imfs*) through repeated iterations based on the extreme points of the data. As seen in the Figure 3, where three *imf* have different frequencies. The overall formula of *imfs* and residuals satisfies the following principle

$$x_t = \sum_i imf_i + res \quad (2)$$

Where *res* is the residual.

However, EMD has a weakness when dealing with mode mixing (Figure 3), where the dataset has multiple oscillatory. EMD cannot separate the inherent features in x_t correctly, resulting in *imf* results that are similar to the original data and fail to capture the features in the dataset (Figure 4).

Therefore, Wu and Huang (2009) introduced EEMD by adding white noise to make the decomposition process more accurate

Table 1: Some other studies of NGP forecasting

References	Methods	Notes
Nguyen and Nabney (2010)	Hybrid MLP and GARCH	using wavelet decomposition
Čeperić et al. (2017)	Combination Neural Network (NN) and SVR	Apply feature selection algorithm
Wang et al. (2020)	Comparison 3 Models SVR, LSTM and Improved Pattern Sequence Similarity Search (IPSS)	The proposed model IPSS performs better than other models
Salehnia et al. (2013)	Comparison Local Linear Regression (LLR), Dynamic Local Linear Regression (DLLR) and Artificial Neural Networks (ANN) models	Combinati on with the Gamma Test
Su et al. (2019)	ANN, Support Vector Machine (SVM), Gradient Boosting Machines, and Gaussian Process Regression (GPR)	ANN show better prediction
Mouchtaris et al. (2021)	Gaussian process regression (GPR), regression trees, support vector machines (SVM), linear regression, and ensemble of trees	Multi-step (1, 3, 5, and 10) days ahead

Figure 2: Example of *n*-step forecasting (source: Lazzeri, 2020, p.5

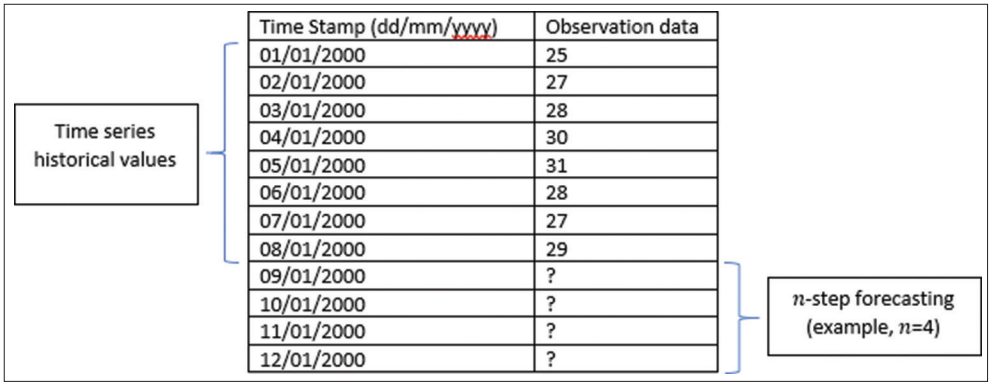

Figure 3: Example application of EMD

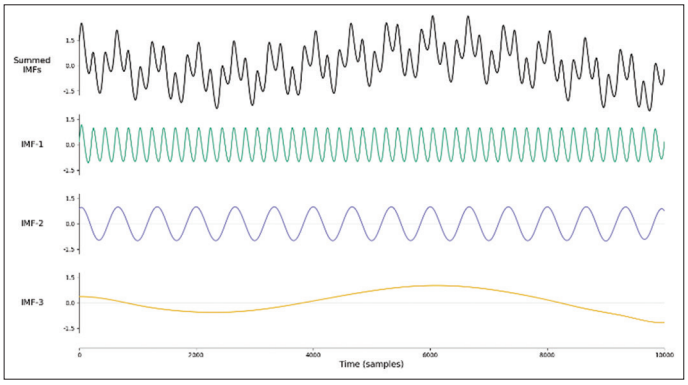

Figure 4: Mode mixing

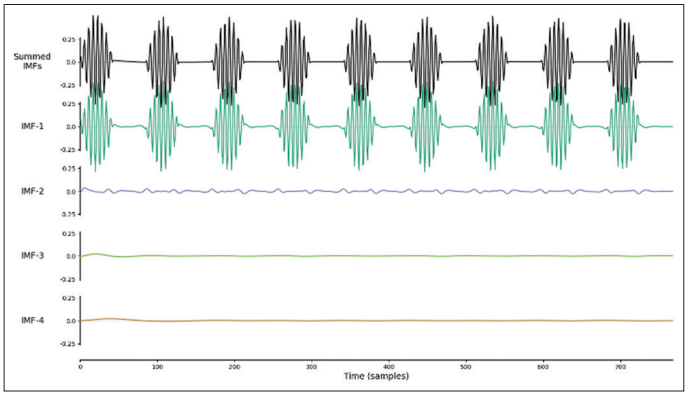

and free from mode mixing. Pseudocode 1 shows the EEMD implementation procedure, where the addition of white noise, $w_n(t) = \sigma \times N(0,1)$, uses a standard deviation (σ) value that adapts to the data value so as not to leave a very large residual. The stopping criterion used is similar to EMD, namely when

a.The number of extreme maxima in envelope (E_t^{up}) and extreme minima in envelope (E_t^{low}) equal to (or +1) to zero crossing

$$N\left(E_t^{up}\right)+N(E_t^{low})-N\left(zero\,crossing\right)\in\{1,0,-1\}$$

b. and, the mean of all E_{up} and E_t^{low} should be 0

$$mean\left(E_t^{up},E_t^{low}\right)\cong 0$$

While the EMD process (on line 6, pseudocode 1.) or $E\cdot(x_t)$ is the following steps: [1] detect the local minimum extrema (min_i) and (max_i), [2] put the minima into the minimum envelope, $min_i \rightarrow E_t^{low}$, and the maxima into another envelope, $max_i \rightarrow E_t^{up}$, [3] interpolate between min_i, also between max_i with cubic splines, [4] determine the value of $E\cdot(x_t)$ from

$$E\cdot\left(x_t\right)=\frac{\left(E_t^{up}+E_t^{low}\right)}{2} \quad (3)$$

Figure 5 shows an example of solving mode mixing with EEMD. The EEMD process on summed *imfs* $(x_t + w_t)$ produces better *imf* scales and is continuous along the time scale. Thus, the problem of mode mixing in the data can be anticipated.

2.2. Long Short-Term Memory (LSTM)

Hochreiter and Schmidhuber (1997) introduced LSTM as an evolution of the previous DL technique, the Recurrent Neural

Network (RNN). LSTM belongs to the category of neural networks well suited to sequential input data with dependencies on previous data. LSTM has advantages over other types of neural networks such as: [1] can learn and store specific parameters, [2] has a fixed model size, [3] has a constant weight value at each node, and [4] is free from exploding and vanishing gradient problems for a massive number of neurons.

Where N = number of LSTM nodes, h_t = hidden state of t, C_t = cell state, $\tilde{C}_t$ = modified cell state, (w_f and b_f), (w_i and b_i), (w_c and b_c), and (w_o and b_o) = weight and bias of forget gate, input-gate, cell-state line, and output-gate, σ (·)= sigmoid activation function, and *tanh(·)*= tanh activation function.

Pseudocode 2 shows the process where LSTM has three main stages: forget-gate, input-gate and output-gate. The analogy of this LSTM model is when a student learns in class. Forget-gate is how much the student still remembers the lessons in the previous class, input-gate is how much the student can understand the lessons received at that time, and output-gate is how much the student remembers today's lessons with past lessons after the end of the class. C_t or cell state shows the long-term influence of the data, while h_{t-1} (hidden state) is the short-term influence of the model.

Pseudocode 1. Ensemble Empirical Mode Decomposition

Given: x_t, $w_t \sim N(0,1)$, *M trials*

Imfs = [ ]
repeat
For *i* in range (*1, M*):

$x_t^i = x_t + w_t^i$

EMD Process -> $E\left(x_t^i\right) = imf_i$

$imf = \frac{1}{M}\sum_{i=1}^{M} imf_i$

imfs.insert (imf)

$x_t^{new} = x_t - imf$

Until stopping criteria is reached

Return *imfs*

Pseudocode 2. Feed-Forward of Long Short-Term Memory

Given: x_t, h_0, C_0, w_f, b_f, w_i, b_i, w_c, b_c, w_0, b_0

imfs = []
For *t* in range (1, *N*):
if t=0, then h_{t-1}=h_0 and C_{t-1}=C_0
#Forget Gate
$f_t = \sigma\,(w_f \cdot [h_{t-1}, x_t] + b_f)$
Input Gate
$i_t = \sigma\,(w_i \cdot [h_{t-1}, x_t] + b_i)$

$\tilde{C}_t = tanh\left(w_c \cdot \left[h_{t-1}, x_t\right] + b_c\right)$

$C_t = f_t * C_{t-1} + i_t * \tilde{C}_t$

Output Gate
$o_t = \sigma\,(w_o \cdot [h_{t-1}, x_t] + b_o)$
$h_t = o_t * tanh\,(C_t)$
end for

Return h_t

LSTM can learn by correcting the weight (w_f, w_i, w_c, w_o) and bias (b_f, b_i, b_c, b_o) values at each iteration, called back-propagation. This stage attempts to bring the prediction model closer to the actual value of the loss function parameter ($\mathscr{L}$).

The weight change occurs in the following formulation

$$w_i^{new} = w_i^{old} - \eta\left(\frac{\partial \nu}{\partial w_i}\right)$$

Where η is the learning rate, and $\frac{\partial \nu}{\partial w_i}$ is the gradient components.

3. RESEARCH METHODOLOGY AND DATA

3.1. Dataset Description

We use natural gas spot price data (Trading Economics, 2022), a dataset based on Henry Hub in Louisiana, United States, interstate natural gas pipeline system contracts using a gas pipeline system traded in 10,000 million British thermal units (USD/mmBtu). Natural gas prices are based on over-the-counter (OTC) and contractual parameters—data range from January 2000 to June 2022 on working days.

Table 2 shows the data range from mean = 4.4813 and standard deviation = 2.216; max data shows 15.378, very far from Q3 percentile = 5.565, indicating that it is susceptible to price spikes. Min data is at 1.482, ranging from Q1 = 1.482.

3.2. Model Description

The forecasting process begins with decomposing the data set x_t using EEMD to produce imf_i. The number of LSTM models is equal to the number i of *imf*. Each $LSTM_i$ will give a forecast output $\hat{x}_{t\cdot i}$ and the final forecast is $\hat{x}_t = \sum_i \hat{x}_{t\cdot i}$

For the *n*-step forecasting process, we use recursive multi-step forecasting, where each step has only one model to predict $\hat{x}_{T+1}, \hat{x}_{T+2}, \ldots, \hat{x}_{T+n}$ with learning data $\{x_t\}$ For *n*-step there will be *n* iterations, i.e. $\{x_1, x_2, \ldots x_T\}$ predicts $\hat{x}_{T+1}$ then $\{x_1, x_2, \ldots x_T, \hat{x}_{T+1}\}$, predicts $\hat{x}_{T+2}$ and so on, so it can be formulated as

$$\left\{\begin{matrix} f\left(x_t\right) = \hat{x}_{T+N} \mid x_t = x_1, \\ x_2, \ldots, x_T, \hat{x}_{T+1}, \ldots, \hat{x}_{T+N-1} \end{matrix}\right\} \forall N \in \{1,2,\ldots,n\} \quad (5)$$

Table 2: Descriptive statistics

Attributes	Natural Gas Price
Count	5742
Mean	4.4813
Standard deviation	2.216
Min	1.482
Max	15.378
25%	2.854
50%	3.872
75%	5.565

3.3. Error Measurement

We use four standard measures of error, *MAE*, *MSE*, *RMSE* and *MAPE* (lower is better), as measures of the success of the forecasting model. *MAE* gives the same weight to small and large gaps, while *MSE* and *RMSE* give a penalty as the error gap increases. For *MAPE*, Lewis (1982) provides categories of forecasting success, where a MAPE value (<10) is classified as a very good forecast, (10 ≤ MAPE < 20) is a good forecast, (20 ≤ MAPE < 50) is a poorly accurate forecast, and (50 ≤ MAPE) is an inaccurate forecast.

$$MAE = \frac{1}{n}\sum_{t=1}^{n}\left|x_t - \hat{x}_t\right| \quad (6)$$

$$MSE = \frac{1}{n}\sum_{t=1}^{n}\left[x_t - \hat{x}_t\right]^2 \quad (7)$$

Figure 5: Example of EEMD

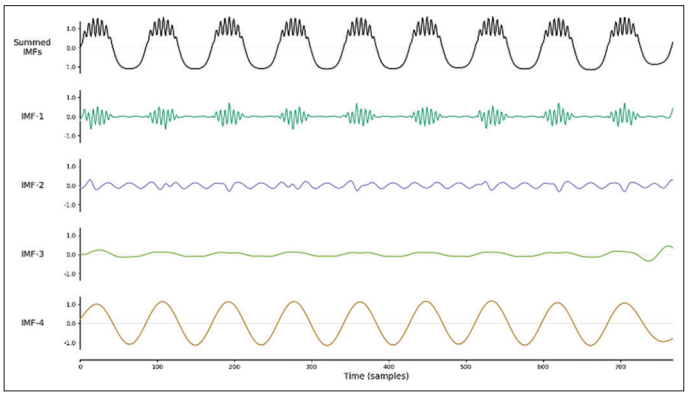

$$RMSE = \sqrt{\frac{1}{n}\sum_{t=1}^{n}\left[x_t - \hat{x}_t\right]^2} \quad (8)$$

$$MAPE = \frac{1}{n}\sum_{t=1}^{n}\left|\left(\frac{x_t - \hat{x}_t}{x_t}\right)100\right| \quad (9)$$

4. RESULTS AND ANALYSIS

4.1. Error Plot Analysis

We use the LSTM model without decomposition as a benchmark for the proposed model. *N*-step forecasting is performed from 30 to 90 steps with an interval of five daily steps, covering short-term (<2 months) to medium-term (more than 2 months). No decomposition model is performed by directly dividing the dataset into training and test data; then, the training data becomes the input of the LSTM model without decomposition. This model is updated every *n* prediction value. The proposed model we built and the NGP dataset are on the git hub link (https://github.com/HerryKG/EEMD_LSTM-Natural-Gas). We use jupyter notebook with python version 3.7.

In Table 3, the measurement error values for all parameters tend to increase as the value of *n* increases due to a significantly different change for predicting data over a more extended period. The MAE value shows that the prediction error for 30-40 steps still has a gap of <0.2, while for (between 40 and 80) steps, the gap value increases from 0.2 to 0.3. With the mean (4.4813), the Q1 (2.854) and the Q3 (5.565), we can assume that the deviation value of 0.2 is small, <7% of the mean. As for the MSE value, since the error value is below 1, the result of the square value of the error will

Figure 6: Proposed model EEMD_LSTM (source: Li et al., 2018)

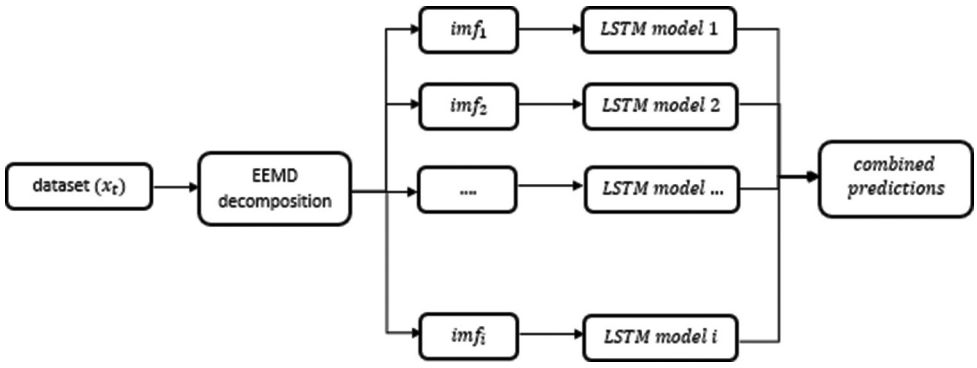

Figure 7: Recursive multi-step forecasting (source: Lazzeri, 2020, p.9)

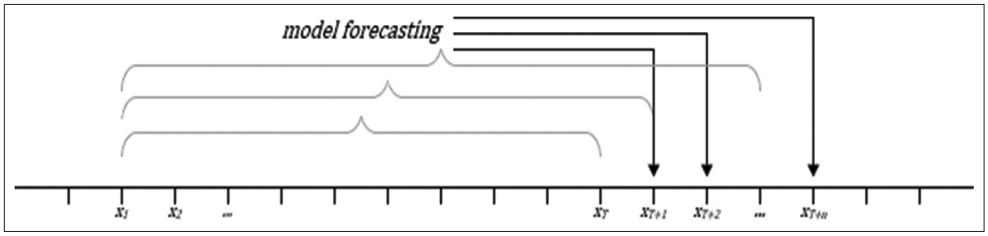

be smaller. Thus, the MSE value is lower than the MAE value, and because most of the errors that occur are still below one, the MSE value will be far below the MAE.

Meanwhile, the RMSE, which is the root square of the MSE, shows how much penalty is imposed compared to no penalty in the MAE. The difference between MAE and RMSE is between 0.1 and 0.13, resulting in the predicted value being very high compared to the actual value. From 30 to 90 steps, most values are below 10 for the MAPE value, which is a very good prediction model.

For the model without decomposition (Table 4), the MAE value for 30-90 steps is higher than the EEMD_LSTM, ranging from 0.36 to 0.72 or more than twice the results for the model with decomposition. The majority of MSE have values above the MAE. These numbers are because most error values are above 1, even at 85 and 90 steps; the MSE and RMSE values are twice the MAE. This condition is far from the results of the decomposition model. As for the MAPE, the value of using no decomposition is about two times bigger than that of using decomposition.

Figures 8-11 show the line plot to represent the measurement error comparison between the EEMD_LSTM and LSTM models in one

Table 3: Error measurement EEMD-LSTM

Number of steps	MAE	MSE	RMSE	MAPE
30-step	0.1788	0.0707	0.2660	5.6597
35-step	0.1876	0.0835	0.2889	5.5974
40-step	0.2097	0.0936	0.3059	6.2046
45-step	0.2235	0.1291	0.3594	6.5376
50-step	0.2553	0.1408	0.3753	7.7791
55-step	0.2623	0.1428	0.3779	8.1613
60-step	0.2758	0.1546	0.3931	8.6936
65-step	0.2769	0.1543	0.3928	8.7806
70-step	0.2890	0.1642	0.4052	9.2052
75-step	0.2940	0.1663	0.4078	9.4663
80-step	0.2970	0.1681	0.4100	9.5536
85-step	0.3105	0.1807	0.4251	10.0751
90-step	0.3269	0.1987	0.4458	10.6936

Table 4: Error measurement no decomposition LSTM

Number of steps	MAE	MSE	RMSE	MAPE
30-step	0.3603	0.3233	0.5686	10.0930
35-step	0.3914	0.3474	0.5894	11.0457
40-step	0.4281	0.4410	0.6641	12.4569
45-step	0.4610	0.4681	0.6842	13.1760
50-step	0.5169	0.5446	0.7380	14.6830
55-step	0.5040	0.6835	0.8267	13.2097
60-step	0.5416	0.7403	0.8604	15.2665
65-step	0.6370	0.7261	0.8521	19.8061
70-step	0.6803	0.8218	0.9065	21.6480
75-step	0.7275	0.9117	0.9548	23.5653
80-step	0.7213	1.2361	1.1118	18.6106
85-step	0.6838	1.2204	1.1047	17.8703
90-step	0.6785	1.3293	1.1529	17.6099

Figure 8: Line plot MAE between EEMD-LSTM and LSTM

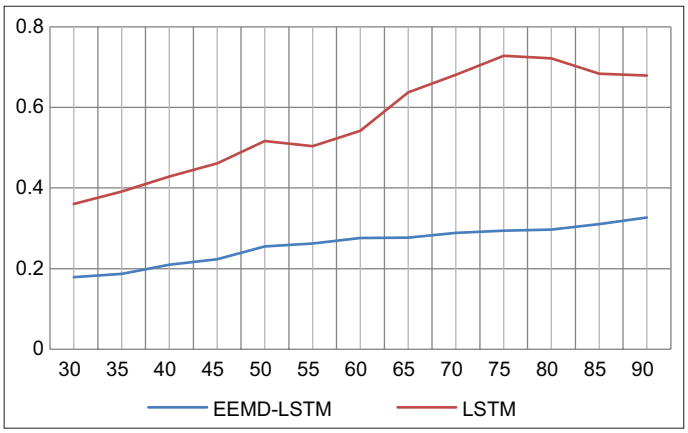

Figure 9: Line plot MSE between EEMD-LSTM and LSTM

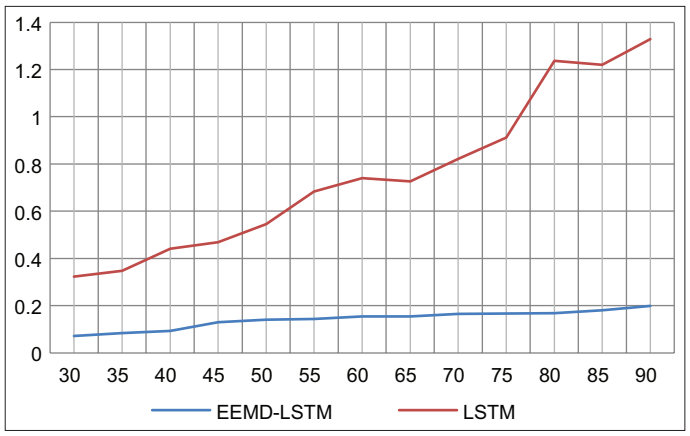

Figure 10: Line plot RMSE between EEMD-LSTM and LSTM

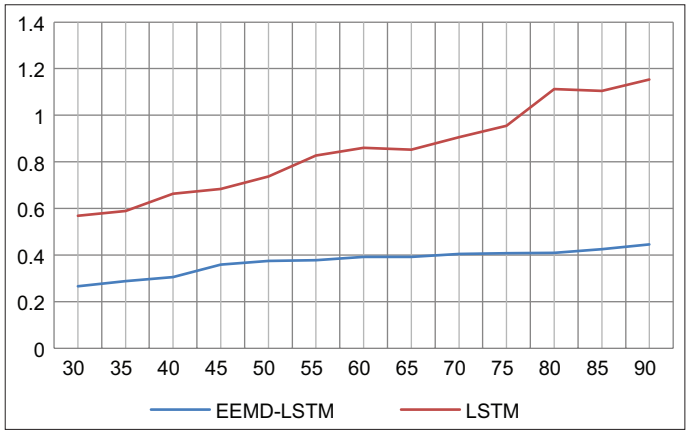

Figure 11: Line plot MAPE between EEMD-LSTM and LSTM

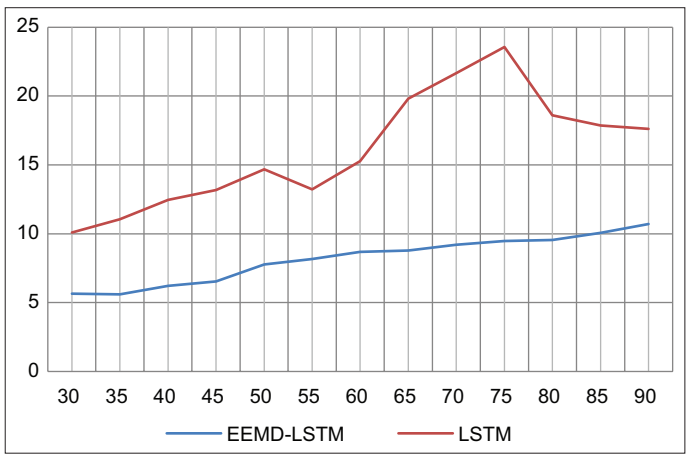

Figure 12: The-box-and-whisker-plot RMSE of EEMD_LSTM

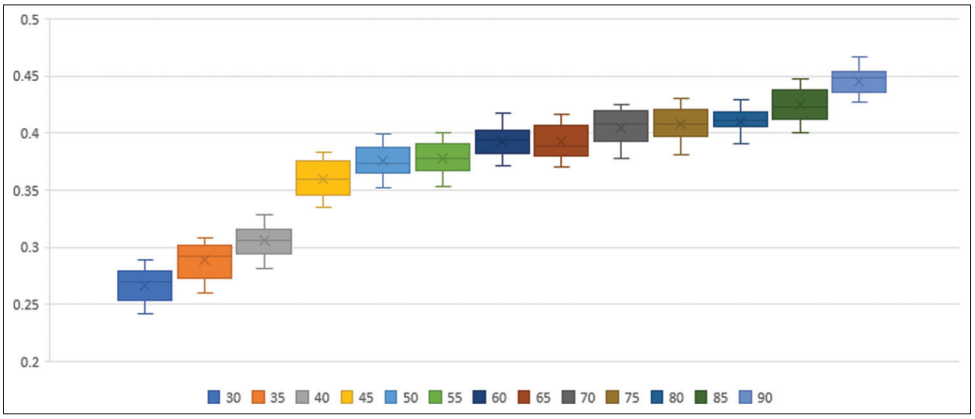

Figure 13: 60-step NGP forecasting using EEMD_LSTM

plot. All parameter errors show lower values for EEMD_LSTM than LSTM. The MAE gap values of the two models show a huge difference, more than six times, consistent with Table 4, where no decomposition has a very extreme error gap compared to EEMD_LSTM. These differences indicate that the decomposition process with EEMD, which separates the *imfs* from the NGP data, can decompose the dataset's features, making it easier for LSTM to predict and avoid very high error gap predictions.

In Figure 11 which shows the MAPE comparison of the two models; it can be seen that the MAPE value for EEMD_LSTM shows the outperforming forecasting model compared to LSTM. The value for EEMD_LSTM shows a value below 10, up to 90 steps, indicating that this forecasting model is robust in the category of very good forecasting. Meanwhile, LSTM has a high spike at 75 steps but drops back to the 15-20 range. Nevertheless, the no-decomposition model can still be classified as a good prediction model.

4.2. Diebold-Mariano Test Analysis

Diebold and Mariano (1995) proposes a test to compare two forecasting models based on error measurement. The p-value shows whether one forecasting model is more accurate than the other and determines the accuracy level.

In Table 5, the P-value varies greatly for several steps, but almost all P-values are >0.01, which is the lowest limit for a model to be significantly accurate with the benchmark model. The larger the *n*-value, the larger the P-value. Above the 60 steps, the accuracy of the EEMD_LSTM model is significantly accurate at a 90% confidence level. Below the 60 steps, the 30, 40 and 55 steps are also significantly accurate at the 90% confidence level, while the 60 step shows significantly accurate at the 95% confidence level. Only the 35 steps have no accuracy because the $P < 0.01$, while the 50 and 45 steps have the significance of accuracy with 99% confidence level.

Table 5: Diebold Mariano test EEMD_LSTM versus LSTM

Number of steps	P-value
30-step	0.1693
35-step	0.0012
40-step	0.1214
45-step	0.0177
50-step	0.0249
55-step	0.1951
60-step	0.0809
65-step	0.0997
70-step	0.121
75-step	0.1365
80-step	0.1408
85-step	0.1506
90-step	0.3367

4.3. Simulation Analysis

One of the disadvantages of the deep learning model is that the output could show different prediction values in each iteration.

This is because the initial weight and bias values (w_o, b_o) are randomly determined. However, we can use the box-and-whisker plot to ensure that the range of the prediction model is robust and provides a stable and accurate prediction value. We have performed 30 simulations of the results of each step with EEMD_LSTM, and we will compare the changes in the RMSE values of each step in the form of plots. In Figure 12 the interquartile range is between 0.01 and 0.025, and the distance between the whiskers is between 0.025 and 0.05; with these values, the difference in RMSE values is still classified as small. With a mean of 4.4813 for the dataset, the change in the predicted value of each dataset based on the whisker distance is approximately 1.11%, while based on the interquartile range, it is 0.56%. These values are still relatively small, and we can conclude that the EEMD_LSTM model is robust.

4.4. Actual versus Prediction Plot

For example, the 60-step in Figure 13 shows that the model's application to the dataset's actual movement looks very good. The EEMD_LSTM model can learn from the dataset and make good predictions. The prediction movement can follow the movement of the dataset, and there is not a very large gap between the prediction and the actual, which can increase the error value very high. Combining decomposition techniques and AI provides satisfactory results in the case of NGP.

5. CONCLUSION

In this study, we present a hybrid technique for NGP forecasting that combines the EEMD decomposition method and the AI deep learning method LSTM. This method has been developed to address the weaknesses of previous techniques. It is applied to the Henry Hub NGP dataset to obtain forecast predictions close to the actual data and reduce measurement errors.

When comparing the proposed model with the non-decomposition model, EEMD_LSTM provides better results for all *n*-step predictions for all measurement error parameters. The comparison of MAE values shows that the non-decomposition model is twice as high as the proposed model. Even for MAPE, EEMD_LSTM falls in the category of very good prediction, where the MAPE value is below 10 (<10). In contrast, the no-decomposition model falls in the lower category, between 10 and 20. This is also confirmed by the Diebold-Mariano test, which shows that the proposed model outperforms the no-decomposition model in all steps. Nine of the 13 prediction steps show significance at the 90% confidence level, with the remainder showing significance between the 95% and 99% confidence levels. This forecasting model has a prediction range value of 1.11% in the box plot simulation analysis. These results show that the proposed model belongs to the robust forecasting category for NGP predictions.

The use of the EEMD decomposition model, in this case, significantly improves forecasting. LSTM has also demonstrated its ability to work well with EEMD to provide 'learning' on data decomposition. The development of forecasting models will continue with the development of decomposition techniques that continue to experience developments, including Complete Ensemble Empirical Mode Decomposition with Adaptive Noise (CEEMDAN) and Wavelet Decomposition. The following study may use a gated recurrent unit (GRU) as a forecasting model.

6. ACKNOWLEDGEMENT

This paper is funded by Stipendium Hungaricum Scholarship by Hungarian Government (Registry Number= SHE-17602-004/2020).

REFERENCES

Agbonifo, P.E. (2016), Natural gas distribution infrastructure and the quest for environmental sustainability in the Niger Delta: The prospect of natural gas utilization in Nigeria. International Journal of Energy Economics and Policy, 6(3), 442-448.

Čeperić, E., Žiković, S., Čeperić, V. (2017), Short-term forecasting of natural gas prices using machine learning and feature selection algorithms. Energy, 140, 893-900.

Cordoni, F. (2020), A comparison of modern deep neural network architectures for energy spot price forecasting. Digital Finance, 2(3-4), 189-210.

Diebold, F.X., Mariano, R.S. (1995), Comparing predictive accuracy. Journal of Business and Economic Statistics, 13, 253-263.

Elgharbawy, A. (2020), A review on natural gas previous, current and forecasting prices and demand. Journal of Petroleum and Mining Engineering, 22(1), 61-64.

Fan, C., Li, Y., Yi, L., Xiao, L., Qu, X., Ai, Z. (2022), Multi-objective LSTM ensemble model for household short-term load forecasting. Memetic Computing, 14(1), 115-132.

Hochreiter, S., Schmidhuber, J. (1997), Long short-term memory. Neural Computation, 9(8), 1735-1780.

Huang, N.E., Shen, Z., Long, S.R., Wu, M.C., Shih, H.H., Yen, N., Tung, C.C., Liu, H.H. (1996), The empirical mode decomposition and the Hilbert spectrum for nonlinear and non-stationary time series analysis. Proceedings of the Royal Society A, 454, 903-995.

Jin, J., Kim, J. (2015), Forecasting natural gas prices using wavelets, time series, and artificial neural networks. PLoS One, 10(11), e0142064.

Lazzeri, F. 2020. Machine learning for time series forecasting with python. Wiley: Indiana, p. 196.

Lewis, C.D. (1982), Industrial and Business Forecasting Methods: A Practical Guide to Exponential Smoothing and curve Fitting. London: Butterworth Scientific Ltd. p40.

Li, C., Tao, Y., Ao, W., Yang, S., Bai, Y. (2018), Improving forecasting accuracy of daily enterprise electricity consumption using a random forest based on ensemble empirical mode decomposition. Energy, 165, 1220-1227.

Liu, D., Sun, K. (2019), Short-term PM2.5 forecasting based on CEEMD-RF in five cities of China. Environmental Science and Pollution Research, 26(32), 32790-32803.

Livieris, I.E., Pintelas, P. (2022), A novel multi-step forecasting strategy for enhancing deep learning models' performance. Neural Computing and Applications, 34(22), 19453-19470.

Lu, Q., Sun, S., Duan, H., Wang, S. (2021), Analysis and forecasting of crude oil price based on the variable selection-LSTM integrated model. Energy Informatics, 4, 47.

Melikoglu, M. (2013), Vision 2023: Forecasting Turkey's natural gas demand between 2013 and 2030. Renewable and Sustainable Energy Reviews, 22, 393-400.

Monjoly, S., André, M., Calif, R., Soubdhan, T. (2019), Forecast horizon and solar variability influences on the performances of multiscale hybrid forecast model. Energies, 12(11), 2264.

Mouchtaris, D., Sofianos, E., Gogas, P., Papadimitriou, T. (2021),

Forecasting natural gas spot prices with machine learning. Energies, 14(18), 5782.

Nguyen, H.T., Nabney, I.T. (2010), Short-term electricity demand and gas price forecasts using wavelet transforms and adaptive models. Energy, 35(9), 3674-3685.

Ozkan, M.B., Karagoz, P. (2015), A novel wind power forecast model: Statistical hybrid wind power forecast technique (SHWIP). IEEE Transactions on Industrial Informatics, 11(2), 375-387.

Perone, G. (2022), Comparison of ARIMA, ETS, NNAR, TBATS and hybrid models to forecast the second wave of COVID-19 hospitalizations in Italy. European Journal of Health Economics, 23(6), 917-940.

Ramyar, S., Kianfar, F. (2019), Forecasting crude oil prices: A comparison between artificial neural networks and vector autoregressive models. Computational Economics, 53(2), 743-761.

Saghi, F., Rezaee, M.J. (2021), An ensemble approach based on transformation functions for natural gas price forecasting considering optimal time delays. PeerJ Computer Science, 7, e409.

Salehnia, N., Falahi, M.A., Seifi, A., Adeli, M.H. (2013), Forecasting natural gas spot prices with nonlinear modeling using Gamma test analysis. Journal of Natural Gas Science and Engineering, 14, 238-249.

Sehgal, N., Pandey, K.K. (2015), Artificial intelligence methods for oil price forecasting: A review and evaluation. Energy Systems, 6(4), 479-506.

Statista Search Department. (2023), Natural Gas Consumption Worldwide from 1998 to 2022 (in Billion Cubic Meters) [Infographic]. Hamburg: Statista. Available from: https://www.statista.com/statistics/282717/global-natural-gas-consumption [Last accessed on 2023 Oct 30].

Su, M., Zhang, Z., Zhu, Y., Zha, D., Wen, W. (2019), Data driven natural gas spot price prediction models using machine learning methods. Energies, 12(9), 1680.

Tamba, J.G., Essiane, S.N., Sapnken, E.F., Koffi, F.D., Nsouandélé, J.L., Soldo, B., Njomo, D. (2018), Forecasting natural gas: A literature survey. International Journal of Energy Economics and Policy, 8(3), 216-249.

Trading Economics. (2022), Natural Gas Summary. In Partnership with the World Bank. Available from: https://tradingeconomics.com/commodity/natural-gas [Last accessed on 2023 Dec 22].

United Nations. (2015), "Paris Agreement". United Nations Treaty Collection. Available from: https://web.archive.org/web/20210705141043, https://treaties.un.org/pages/viewdetails.aspx?src=treaty&mtdsg_no=xxvii-7-d&chapter=27&clang=_en [Last accessed on 2023 Oct 15].

Wang, J., Lei, C., Guo, M. (2020), Daily natural gas price forecasting by a weighted hybrid data-driven model. Journal of Petroleum Science and Engineering, 192, 107240.

Wang, W.C., Chau, K.W., Xu, D.M., Chen, X.Y. (2015), Improving forecasting accuracy of annual runoff time series using ARIMA based on EEMD decomposition. Water Resources Management, 29(8), 2655-2675.

Wu, Z., Huang, N.E. (2009), Ensemble empirical mode decomposition: A noise-assisted data analysis method. Advances in Adaptive Data Analysis, 1(1), 1-41.

Yan, K., Wang, X., Du, Y., Jin, N., Huang, H., Zhou, H. (2018), Multi-step short-term power consumption forecasting with a hybrid deep learning strategy. Energies, 11(11), 3089.

Zamani, N. (2016), How the crude oil market affects the natural gas market? Demand and supply shocks. International Journal of Energy Economics and Policy, 6(2), 217-221.

Zhang, H., Xu, H.R., Peng, G.S., Qian, Y.D., Zhang, X.X., Yang, G.L., Shen, C., Li, Z., Yang, J.W., Wang, Z.Q., He, F., Gu, C.L., Zhu, M.B. (2022), A prediction model of relativistic electrons at geostationary orbit using the EMD-LSTM network and geomagnetic indices. Space Weather, 20(10), 1-12.